Theoretical investigation of hierarchical sub-wavelength photonic structures fabricated using high-order waveguide-mode interference lithograph*

Ru Wang(王茹)[1], Xiangxian Wang(王向贤)[1,†], Hua Yang(杨华)[1], and Yunping Qi(祁云平)[2]

[1] School of Science, Lanzhou University of Technology, Lanzhou 730050, China
[2] College of Physics and Electronic Engineering, Northwest Normal University, Lanzhou 730070, China

(Received 9 September 2016; revised manuscript received 29 October 2016; published online 20 December 2016)

This paper presents the theoretical investigation of hierarchical sub-wavelength photonic structures with various periods and numbers of layers, which were fabricated using a high-order waveguide-mode interference field. A 442-nm laser was used to excite high-order waveguide modes in an asymmetric metal-cladding dielectric waveguide structure. The dispersion curve of the waveguide modes was theoretically analyzed, and the distribution of the interference field of high-order waveguide modes was numerically simulated using the finite-element method. The various dependences of the characteristics of hierarchical sub-wavelength photonic structures on the thickness and refractive index of the photoresist and the waveguide mode were investigated in detail. These hierarchical sub-wavelength photonic structures have various periods and numbers of layers and can be fabricated by a simple and low-cost method.

Keywords: sub-wavelength photonic structure, finite-element method, waveguide modes, lithography

PACS: 42.25.Hz, 42.50.St, 42.79.Gn **DOI:** 10.1088/1674-1056/26/2/024202

1. Introduction

Micro- and nanostructures of various shapes and sizes have tremendous prospects for applications in diverse fields, including physics,[1–3] material science,[4,5] chemistry,[6,7] and medical science.[8] One-dimensional sub-wavelength gratings can be used to enhance Raman scattering intensity.[9] Patterning of TiO_2[10] nanostructures, for which geometries and spacings can be precisely controlled, may play an important role in the improvement of sensors for gas detection. Different methods[11] have been used to fabricate micro- and nanostructures for research and applications. Electron beam lithography,[12,13] atomic force microscope lithography,[14] UV photolithography,[15] and x-ray lithography[16] are the most commonly used fabrication methods. These methods all present disadvantages, such as complicated techniques, high costs, and low yields.

Recently, Radwanul Hasan Siddique[17] *et al.* demonstrated the fabrication of hierarchical photonic nanostructures, which utilized the laser interference pattern in the vertical direction in addition to the conventional horizontal one. They found that the structural color of the final photonic structure can be influenced directly by various factors, including the period of the vertical standing wave and the photoresist material. Although they demonstrated that the method has an advantage for photonic nanostructures with nanoscale elements in the vertical direction, the period of the photonic nanostructures was not sub-wavelength in the horizontal direction.

Here, we present a theoretical approach showing that high-order waveguide-mode interference lithography can fabricate hierarchical sub-wavelength photonic structures (HSPS) in both the vertical and horizontal directions. Furthermore, this method supports fabrication of sub-wavelength photonic structures with different periods and layers. This HSPS nanolithography method is simple, low-cost, and maskless.

2. Theoretical analysis

Figure 1(a) shows a schematic of the lithographic system. Here, the system configuration, which is similar to one that we reported previously, supports fabrication of a sub-wavelength grating by utilizing the low-order waveguide mode interference lithography technique[18,19] and is based on an asymmetric metal-cladding dielectric waveguide structure. An index-matching oil is used to connect the glass substrate and prism. The refractive index (RI) of the index-matching oil and the glass substrate are similar to the RI of the prism. A laser beam is split into two identical beams with a beam splitter. The resulting beams then are reflected into the prism using two mirrors. When the two laser beams irradiate the sample at an angle θ_m at which high-order waveguide modes are excited, two waveguide modes are generated. In the photoresist layer,

*Project supported by the National Natural Science Foundation of China (Grant No. 61505074), the National Key Basic Research Program of China (Grant No. 2013CBA01703), and the HongLiu Young Teachers Training Program Funded Projects of Lanzhou University of Technology (Grant No. Q201509).

†Corresponding author. E-mail: wangxx869@126.com

© 2017 Chinese Physical Society and IOP Publishing Ltd

one mode propagates to the left, and another propagates to the right. The interference between the two waveguide modes creates standing waves, which are used to inscribe HSPS. The photoresist layer employs a positive photoresist. After the exposure and developing processes, HSPS are fabricated. Figure 1(b) shows the enlarged schematic view of the inscribed HSPS inscribed; the x–y plane lies along the interface of the Ag and photoresist layer, and the z axis points to the air from the photoresist.

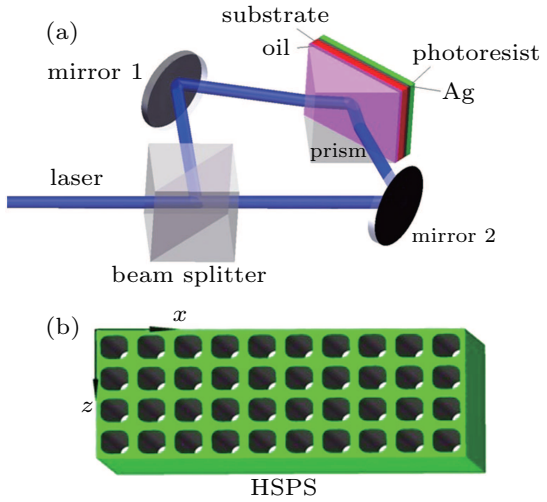


Fig. 1. (color online) (a) Schematic diagram of the lithographic system configuration based on an asymmetric metal-cladding dielectric waveguide structure. (b) Enlarged schematic view of the inscribed HSPS.

The eigenmode equation of the asymmetric metal-cladding dielectric waveguide structure can be expressed as[20]

$$\kappa_2 d = m\pi + \arctan\left(\rho_1 \frac{\alpha_3}{\kappa_2}\right) + \arctan\left(\rho_2 \frac{\alpha_1}{\kappa_2}\right), \tag{1}$$

where m is the mode-order index, d is the thickness of the photoresist, and κ_2, α_1, and α_3 can be expressed as

$$\begin{cases} \kappa_2 = \left(k_0^2\varepsilon_2 - \beta^2\right)^{1/2}, \\ \alpha_1 = \left(\beta^2 - k_0^2\varepsilon_1\right)^{1/2}, \\ \alpha_3 = \left(\beta^2 - k_0^2\varepsilon_3\right)^{1/2}. \end{cases} \tag{2}$$

Here, β is the propagation constant and $k_0 = 2\pi/\lambda_0$ is the wavenumber corresponding to wavelength λ_0 in a vacuum. Furthermore, ρ_1 and ρ_2 are given by

$$\rho_1 = \begin{cases} 1, & \text{for TE modes,} \\ \varepsilon_2/\varepsilon_3, & \text{for TM modes,} \end{cases} \tag{3}$$

and

$$\rho_2 = \begin{cases} 1, & \text{for TE modes,} \\ \varepsilon_2/\varepsilon_1, & \text{for TM modes,} \end{cases} \tag{4}$$

respectively, where ε_1 is the dielectric constant of Ag. Because the imaginary part of ε_1 is much less than its real part,[21,22] the imaginary part, for the sake of convenience, can be neglected in the analysis. Similarly, ε_2 and ε_3 are the dielectric constants of the photoresist and air, respectively. In this structure, the allowed range of the effective RI for the waveguide modes is

$$\sqrt{\varepsilon_3} < \beta_m/k_0 < \sqrt{\varepsilon_2}. \tag{5}$$

Moreover, the coupling excitation of high-order waveguide modes should satisfy the wave vector-matching condition, which is defined by

$$k_0 n_0 \sin\theta_m = \beta_m, \tag{6}$$

where n_0 is the prism RI and θ_m is the resonance angle of the m-order waveguide mode. Furthermore,

$$n_0 \sin\theta_m = n_{\text{eff}} = \sqrt{\varepsilon_0}\sin\theta_m, \tag{7}$$

where n_{eff} is the effective RI of the waveguide modes.

When one uses the above-mentioned asymmetric metal-cladding dielectric waveguide structure, the period of HSPS inscribed in the x direction can be expressed as

$$\Delta x = \frac{\lambda_0}{2n_{\text{eff}}} = \frac{\lambda_0}{2\sqrt{\varepsilon_0}\sin\theta_m} = \frac{\pi}{\beta_m}. \tag{8}$$

The number layers of HSPS, which depends on the order of the exciting waveguide modes, is determined in the z direction. Theoretical analysis of the dispersion curve and the distribution of the interference field of high-order waveguide modes by the finite-element method demonstrates that the layer number of HSPS is equal to the mode-order index plus 1, that is $m+1$.

3. Numerical results

Equation (8) shows that the HSPS period is determined by λ_0 of the incident light, the prism RI, and θ_m. Combining Eq. (1) through Eq. (6), θ_m can be determined from the dispersion curve, which can be calculated by using relative parameters, namely, the waveguide mode index, the incident light wavelength, and the RI and thickness of both the metal and photoresist. In this study, we used a 442-nm laser as the exciting light source and an Ag film as the metal layer. The dielectric constant of Ag is $-5.7018 + 0.7514\mathrm{i}$[23] at 442 nm. A 45-nm-thick Ag film was considered in the calculations.

When the prism RI is 1.6 and the photoresist RI and thickness are 1.7 and 950 nm, respectively, the θ_m values of the TE_5 and TM_5 waveguide modes are 45° and 50°, respectively. The periods of HSPS inscribed by the TE_5 and TM_5 waveguide modes are 196 nm and 180 nm, respectively. The calculated results of the periods for HSPS align with the results obtained from the simulation. Figures 2(a) and 2(b) show the simulated electric field $|E_y|$ of the TE_5 waveguide-mode interference and the magnetic-field component $|H_y|$ of the TM_5 waveguide-mode interference in the multilayer film, respectively.

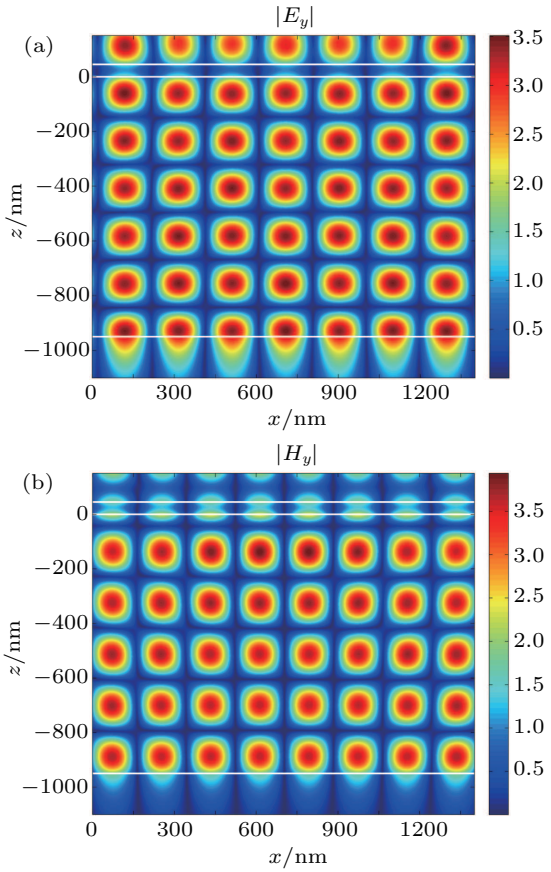


Fig. 2. (color online) (a) Simulated electric field $|E_y|$ of TE_5 waveguide-mode interference. (b) The simulated magnetic-field component $|H_y|$ of TM_5 waveguide-mode interference. The white lines indicate the interfaces of glass, Ag, photoresist, and air, from top to bottom. The prism RI is 1.6, and the photoresist RI and thickness are 1.7 and 950 nm, respectively.

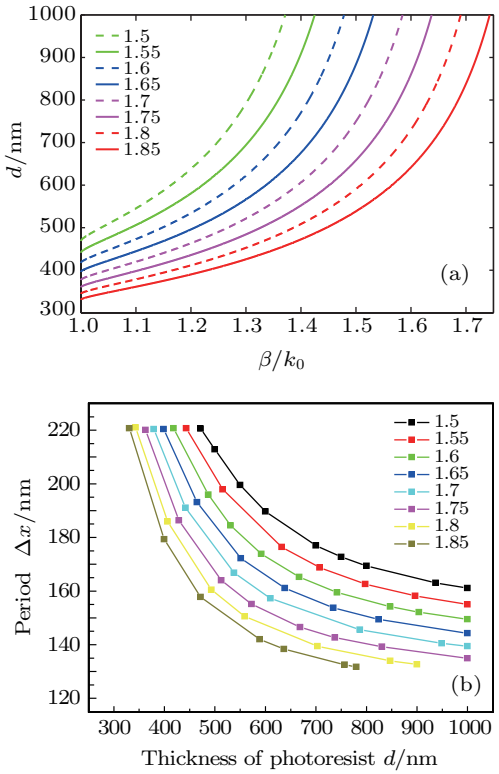


Fig. 3. (color online) (a) Dispersion curves for TE_2 modes for different values of photoresist RI. (b) The relationship between HSPS period and photoresist thickness with different values of photoresist RI using TE_2-mode interference. The prism RI is 1.7.

3.1. Photoresist thickness and RI

The proposed method can fabricate HSPS with various periods. In pursuit of this outcome, we investigated in detail the various dependences of HSPS characteristics on the photoresist thickness and RI, and on the waveguide modes. As shown in Eq. (8), the HSPS period is inversely proportional to β_m. Therefore, we first studied the dispersion curves of TE_2 modes using different RIs for the photoresist while maintaining the prism RI at 1.7.

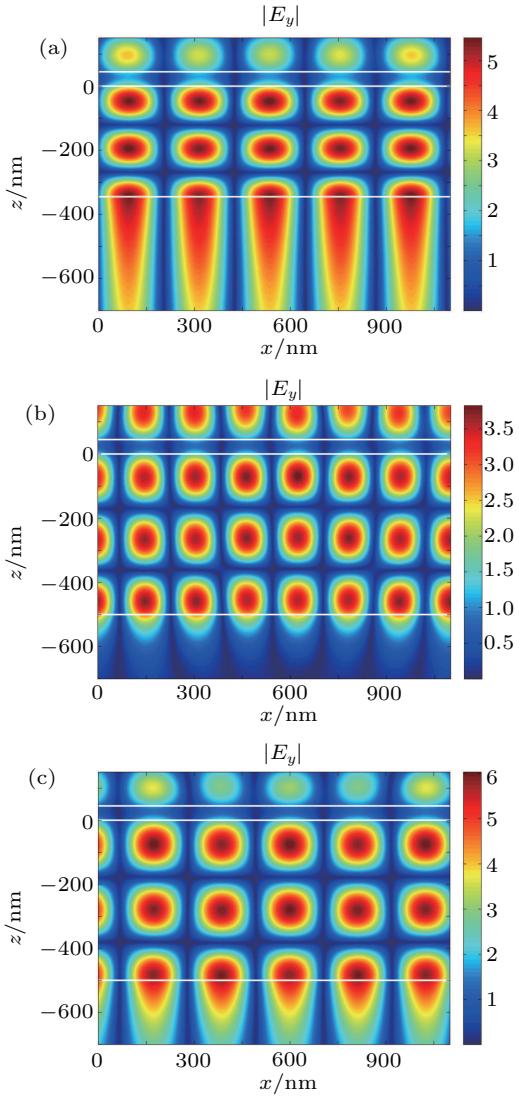


Fig. 4. (color online) Simulated electric field $|E_y|$ of TE_2-mode interference in multilayer film. The white lines indicate the interfaces of glass, Ag, photoresist, and air, from top to bottom. (a) Values of the prism and photoresist RI are 1.7 and 1.8, respectively; the photoresist thickness is 345 nm. (b) The values of RI for prism and photoresist are the same as in (a); the photoresist thickness is 500 nm. (c) The values of the prism and photoresist RI are 1.7 and 1.5, respectively, and the photoresist thickness is 500 nm.

Figure 3(a) shows the calculated dispersion curve. With the same photoresist RI, β_m is larger for thicker photoresists, yielding smaller HSPS periods. With the same photoresist thickness, the larger the photoresist RI, the larger the β_m value and the smaller the HSPS period. Figure 3(b) exhibits the relationships among the HSPS period, photoresist thickness,

and RI. The HSPS period decreases as the photoresist thickness increases. Figures 4(a) and 4(b) show $|E_y|$ for the TE_2 waveguide-mode interference for photoresist thicknesses of 345 nm and 500 nm, respectively, where the prism and photoresist RIs are 1.7 and 1.8, respectively. HSPS periods are 221 nm and 159 nm when the photoresist thicknesses are 345 nm and 500 nm, respectively. When the prism RI is 1.7 and the photoresist thickness and RI are 500 nm and 1.5, respectively, the HSPS period is 213 nm. This HSPS period is larger than when the RI is 1.8. Figure 4(c) shows $|E_y|$ for TE_2 waveguide-mode interference when the photoresist RI and thickness are 1.5 and 500 nm, respectively. The results clearly demonstrate that a larger photoresist RI will yield an inscription of HSPS with a smaller period, as shown in Fig. 3(b). The TM modes also follow the same trend. Thus, HSPS with various periods can be fabricated by varying the photoresist thickness or RI.

3.2. Waveguide modes

The value of β_m also depends on the polarization and m. Figure 5(a) shows the dispersion curves for different waveguide modes when the photoresist RI is 1.7. If the photoresist thickness and RI are constant, β_m is larger for m-order TM modes than for same-order TE modes. Therefore, the period of HSPS inscribed using m-order TM modes is smaller than the HSPS period inscribed using TE modes. For the same

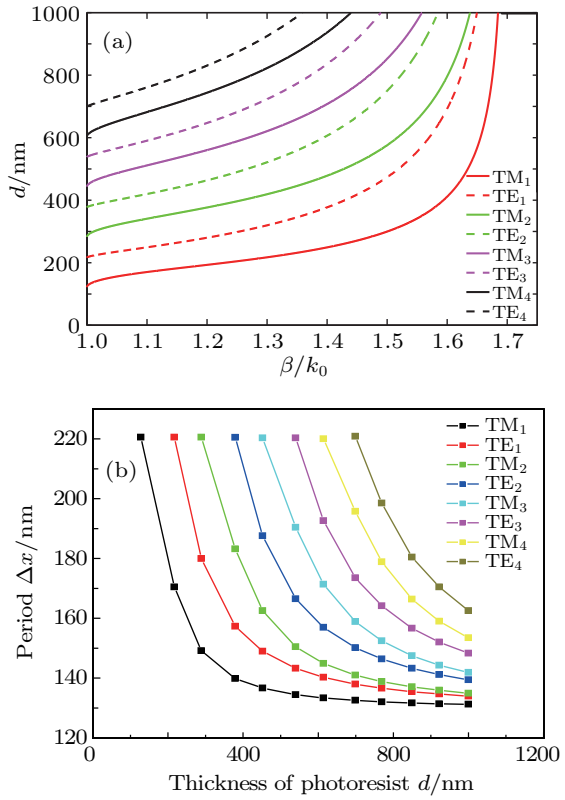


Fig. 5. (color online) (a) Dispersion curves for different waveguide modes with photoresist RI 1.7. (b) The relationship between HSPS period and photoresist thickness for different waveguide modes. Here, the RI for the photoresist and prism are 1.7 and 1.85, respectively.

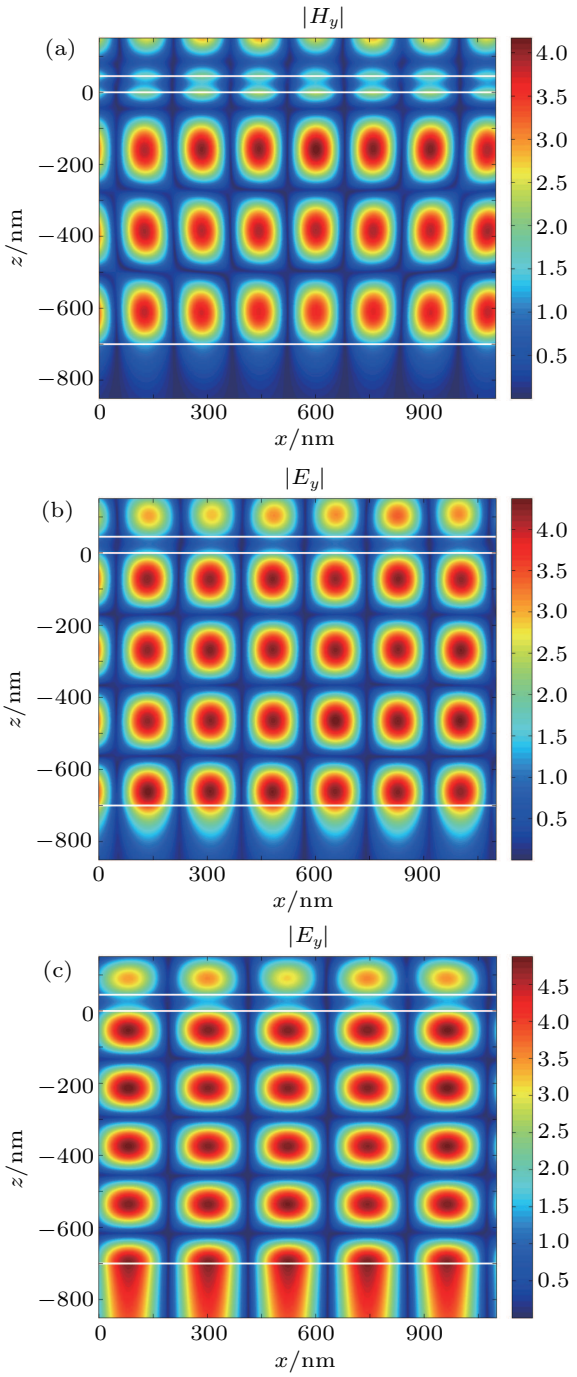


Fig. 6. (color online) (a) Simulated magnetic-field component $|H_y|$ of TM_3-mode interference in multilayer film. The simulated electric fields $|E_y|$ of (b) TE_3- and (c) TE_4-mode interference in multilayer films. The white lines indicate the interfaces of glass, Ag, photoresist, and air, from top to bottom. The prism RI is 1.85, and the photoresist RI and thickness are 1.7 nm and 700 nm, respectively.

polarization modes, when the photoresist thickness and RI are identical, β_m is larger for low-order waveguide modes than for high-order ones. This characteristic implies that the HSPS period is smaller in the former case than in the latter. Figure 5(b) shows the relationship between the HSPS period and the photoresist thickness for different waveguide modes with prism RI 1.85. Figure 6(a) shows $|H_y|$ for TM_3-mode interference in the multilayer film for an HSPS period of 159 nm. Figures 6(b) and 6(c) present $|E_y|$ for TE_3- and TE_4-mode inter-

ference, which can inscribe HSPS with periods of 173 nm and 221 nm, respectively. The photoresist thickness was considered to be 700 nm in the simulation. The values of RI for the photoresist and prism are identical to those shown in Fig. 5(b). These results indicate the possibility of selecting appropriate waveguide modes to write HSPS with a required period and number of layers. Thus, HSPS with various periods and different numbers of layers can be fabricated.

4. Conclusion

We theoretically demonstrated hierarchical sub-wavelength photonic structures fabricated using an asymmetric metal-cladding dielectric waveguide structure. HSPS with various periods and layers can be fabricated using this method. Furthermore, HSPS can be controlled effectively using the excited waveguides modes and photoresist parameters, in particular, the photoresist thickness, which can be easily changed when performing experiments. Our analysis of the interference field distribution of the high-order waveguide-modes indicates that a positive photoresist should be used to fabricate hierarchical sub-wavelength photonic structures for experimental uses. The HSPS fabrication method presented here is both simple and low-cost; it provides a possible experimental method for fabricating hierarchical sub-wavelength photonic structures.

References

[1] Wen F, David S, Checoury X, Kurdi M E and Boucaud P 2008 *Opt. Express* **16** 12278

[2] Antos R and Veis M 2010 *Opt. Express* **18** 27511

[3] Ma Y W, Wu Z W, Zhang L H, Liu W F and Zhang J 2015 *Chin. Phys. Lett.* **32** 94202

[4] Singh J P, Karabacak T, Ye D X and Liu D L 2005 *J. Vac. Sci. Technol. B.* **23** 2114

[5] Zhao Y P, Chaney S B and Zhang Z Y 2006 *J. Appl. Phys.* **100** 063527

[6] Geng Z, Zhang Y, Yuan X, Huo M, Zhao Y, Lu Y and Qiu Y 2015 *J. Alloys Compd.* **644** 734

[7] Li X, Hu Z, Liu J, Li D, Zhang X, Chen J and Fang J 2016 *Appl. Catal. B-Environ.* **195** 29

[8] Hu M, Chen J Y, Li Z Y, Au L, Hartland G V, Li X, Marquez M and Xia Y 2006 *Chem. Soc. Rev.* **35** 1084

[9] Khorasaninejad M, Walia J and Saini S S 2013 *Appl. Phys. Lett.* **103** 163110

[10] Hotovy I, Kostic I, Nemec P, Predanocy M and Rehacek V 2015 *J. Micromech. Microeng.* **25** 074006

[11] Xie Z, Yu W, Wang T S, Zhang H X, Fu Y Q, Liu H, Li F Y, Lu Z W and Sun Q 2011 *Plasmonics* **6** 565

[12] Ivo U, Patrik H and John M 2008 *J. Vac. Sci. Technol. B* **26** 1197

[13] Gunnarsson L, Rindzevicius T, Prikulis J, Kasemo B, Kall M, Zou S and Schatz G C 2005 *J. Phys. Chem. B* **109** 1079

[14] Chien F S S, Wu C L, Chou Y C, Chen T T, Gwol S and Hsieh W F 1999 *Appl. Phys. Lett.* **75** 2429

[15] Bogaerts W, Wiaux V, Taillaert D, Beckx S, Luyssaert B and Bienstman P 2002 *IEEE J. Selec. Top. Quantum Electron.* **8** 928

[16] Feiertag G, Ehrfeld W, Freimuth H, Kolle H, Lehr H, Schmidt M, Sigalas M M, Soukoulis C M, Kiriakidis G, Pedersen T, Kuhl J and Koenig W 1997 *Appl. Phys. Lett.* **71** 1441

[17] Siddique R H, Hunig R, Faisal A, Lemmer U and Holscher H 2015 *Opt. Mater. Express* **5** 996

[18] Wang X, Zhang D, Chen Y, Zhu L, Yu W, Wang P, Yao P, Ming H, Wu W and Zhang Q 2013 *Appl. Phys. Lett.* **102** 031103

[19] Wang R, Wang X X, Yang H and Ye S 2016 *Acta. Phys. Sin.* **65** 094206 (in Chinese)

[20] Kaminow L P, Mammel W L and Weber H P 1974 *Appl. Opt.* **13** 396

[21] Lu H, Cao Z, Li H and Shen Q 2004 *Appl. Phys. Lett.* **85** 4579

[22] Li H, Cao Z, Lu H and Shen Q 2003 *Appl. Phys. Lett.* **83** 2757

[23] Palik E D 1991 *Handbook of Optical Constants of Solids* (Academic Press)